THE ASTROPHYSICAL JOURNAL, 465:L95–L98, 1996 July 10

C IV ABSORPTION FROM GALAXIES IN THE PROCESS OF FORMATION

MARTIN G. HAEHNELT,[1] MATTHIAS STEINMETZ,[1, 2] AND MICHAEL RAUCH[3, 4]
Received 1995 December 21; accepted 1996 April 25

ABSTRACT

We investigate the heavy element QSO absorption systems caused by gas condensations at high redshift that evolve into galaxies at the present epoch. Artificial QSO spectra were generated for a variety of lines of sight through regions of the universe simulated with a hydrodynamics code. The C IV and H I absorption features in these spectra closely resemble observed C IV and H I absorption systems if [C/H] ~ -3 to -2 is assumed. C IV absorption complexes with multiple-component structure and velocity spreads up to $\sim$600 km s^{-1} are found. The broadest systems are caused by lines of sight passing through groups of protogalactic clumps aligned along filamentary structures expanding with the Hubble flow. Typical clumps have a radius of about 5–10 kpc, a baryonic mass of $\sim 10^9\ M_\odot$, and are surrounded by hot gas atmospheres with a radius of about 30 kpc. The temperature of a considerable fraction of the gas does not take the photoionization equilibrium value. This invalidates density and size estimates derived from thermal equilibrium models. Our model may be able to explain both high-ionization multicomponent heavy-element absorbers and damped Lyα systems as groups of small protogalactic clumps.

Subject headings: cosmology: observations — cosmology: theory — galaxies: evolution — galaxies: formation — intergalactic medium — quasars: absorption lines

1. INTRODUCTION

Heavy element absorption as seen in the spectra of distant quasi-stellar objects (QSOs) is commonly thought to be produced by metal-contaminated gas associated with galaxies. At low and intermediate redshifts, a connection of low-ionization metal absorption systems with observable galaxies is strongly indicated by successful searches for galaxies close to the absorption redshift (Bergeron 1986; Bergeron & Boissé 1991; Lanzetta et al. 1995; Steidel 1995).

However, such a close one-to-one correspondence between galaxy and absorption system need not be valid for higher ionization (C IV) systems at higher redshifts (York 1988). Several features, like the extended component structure of C IV–selected absorption systems, are equally difficult to understand in terms of a stationary cloudlet-in-halo model, as in terms of absorption along lines of sight (LOSs) through known types of local galaxy clusters (Pettini et al. 1983; Morris et al. 1986; Mo 1994). Instead, going back in time, we should ultimately see the small-scale gas condensations from which instabilities and hierarchical clustering have built up present-day galaxies (Lake 1988; Steidel 1990).

Numerical simulations of the large-scale distribution of neutral hydrogen have recently led to a major advance in the understanding of Lyα absorption systems (Cen et al. 1994; Petitjean, Mücket, & Kates 1995; Hernquist et al. 1996). Here we investigate smaller scales in order to understand the nature of heavy element absorption systems. We have used a set of smoothed particle hydrodynamics (SPH) simulations to model the detailed evolution of regions that by the present epoch contain one to three galaxies with halo circular velocities between 100 and 200 km s^{-1}. We focus on the C IV absorption properties of these regions. Recent spectroscopic studies by Tytler et al. (1995) and Cowie et al. (1995) indicate that all baryonic matter at the relevant redshift could be contaminated with heavy elements to some degree. For simplicity, we assume in the present paper a small homogeneously distributed fraction of metals.

In § 2 we describe the technical details of the SPH simulations and of our determination of the ionization state of carbon. Section 3 illustrates the characteristic features of C IV absorption in our simulations, and in § 4 we discuss some implications.

2. THE SPATIAL DISTRIBUTION OF NEUTRAL HYDROGEN AND C IV

2.1. *Simulating the Gas Distribution*

The simulations were performed using GRAPESPH (Steinmetz 1996). The cosmological background model is a $\Omega = 1$, $H_0 = 50$ km s^{-1} Mpc^{-1} cold dark matter (CDM) cosmogony with a normalization of $\sigma_8 = 0.63$. The baryon fraction is $\Omega_b = 0.05$. The mass resolution is $(0.5\text{–}2) \times 10^7\ M_\odot$ for the gas. The gravitational softening is 1.25–2.5 kpc for the gas and a factor of 2 larger for the dark matter. The simulations cover a high-resolution sphere with a radius of about 2–4 Mpc. The tidal field due to surrounding matter was taken into account using the multimass technique described in Navarro, Frenk, & White (1995). For the UV background, we assume the redshift dependence given by Vedel, Hellsten, & Sommer-Larsen (1994),

$$J(\nu) = 10^{-21} \left[1 + \left(\frac{5}{1+z}\right)^4\right]^{-1} \times \left(\frac{\nu}{\nu_{\rm H}}\right)^{-\alpha} \text{ergs s}^{-1}\ \text{cm}^{-2}\ \text{Hz}^{-1}\ \text{sr}^{-1}\,, \quad (1)$$

[1] Max-Planck-Institut für Astrophysik, Karl-Schwarzschild-Straße 1, Garching, Germany; mhaehnelt@mpa-garching.mpg.de, msteinmetz@mpa-garching.mpg.de.
[2] Present address: Department of Astronomy, University of California, Berkeley, Berkeley 94720.
[3] Astronomy Department, 105-24 California Institute of Technology, Pasadena 91125; mr@astro.caltech.edu.
[4] Hubble Fellow.

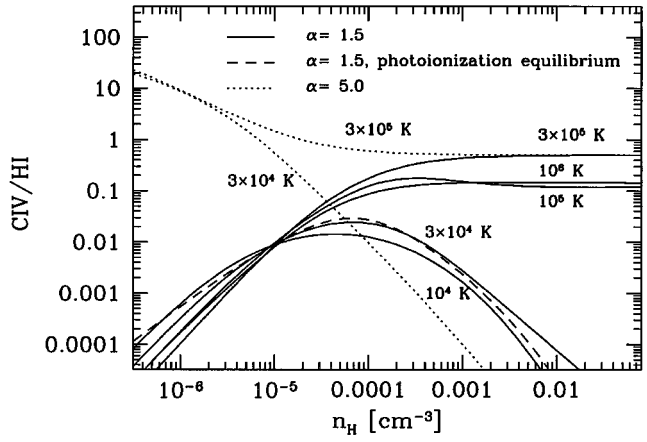

FIG. 1*a*

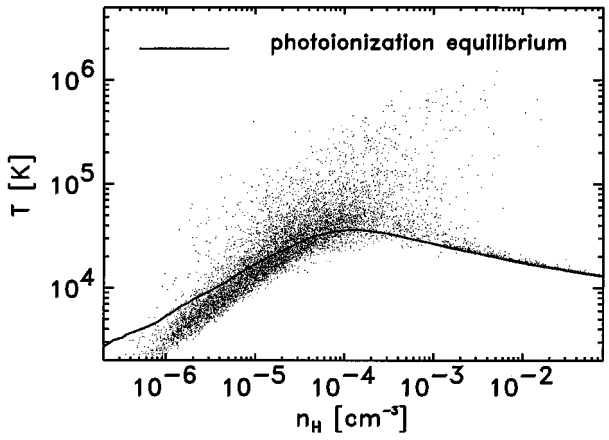

FIG. 1*b*

FIG. 1.—(*a*) Column density ratio C IV/H I as function of density for [C/H] = −2 and a UV background with $J_{-21} = 0.3$ and spectral index $\alpha = 1.5$ beyond the Lyman edge (*solid curves*). Calculations were done with CLOUDY for fixed temperatures. For the dashed curve, the temperature is determined by photoionization equilibrium. The dotted curves are for an extremely soft spectrum with $\alpha = 5$. (*b*) A typical temperature/density distribution for the gas particles in our SPH simulations. The solid curve shows the corresponding relation assuming photoionization equilibrium.

where ν_H is the frequency corresponding to the ionization energy of hydrogen (13.6 eV). For α, a value of 1.5 was usually assumed.

2.2. *The Ionization State of the Gas*

We have used the photoionization code CLOUDY to calculate the ionization state of carbon (Ferland 1993). CLOUDY was used in its "Lyα absorber mode." The solid curves in Figure 1*a* show the column density ratio of C IV to neutral hydrogen for [C/H] = −2, a UV background given by equation (1) with $\alpha = 1.5$ and $z = 3$, and a fixed temperature as indicated on the plot. For the dashed curve, the temperature was assumed to be determined by photoionization equilibrium. Figure 1*b* shows a typical scatter plot of density versus temperature of the SPH particles in our simulations. Around the peak of the equilibrium curve, the temperature is generally larger than the equilibrium value because of compressional heating. Also seen is a modest deviation from the equilibrium curve toward smaller temperatures due to adiabatic cooling at the lowest densities.

3. ABSORPTION SPECTRA

3.1. *General Appearance of Absorption Features*

In Figures 2 and 3 we show artificial spectra that were produced with a signal-to-noise ratio of 50, an instrumental broadening of 8 km s^{-1}, and a bin size of 2 km s^{-1} to match the spectral resolution obtainable with the HIRES spectrograph of the Keck telescope. A Voigt profile with optical depth and width corresponding to its temperature and column density was generated for each volume element in the box. The contributions from all such individual profiles to the optical depth in a given velocity bin where then co-added to produce the full spectrum. H I and C IV are overplotted in velocity space. For clarity, we plot only the λ1548 line of the C IV doublet.

The spectra generally show a convincing resemblance both to the weak C IV absorption systems observed, e.g., by Cowie et al. (1995) and others and the stronger variants seen in low-resolution C IV surveys (e.g., Sargent, Boksenberg, & Steidel 1988). Figure 2 shows the H I and C IV absorption for a 5 × 5 mosaic of LOSs around a filamentary structure at $z = 3$. The proper distance between the panels is 10 kpc. The LOS at the center penetrates about 5 to 7 different clumps (see also Fig. 3*b*) producing a prominent cluster of C IV lines. The clustering pattern varies considerably over scales of 5 kpc. At a distance of about 30 kpc, the C IV absorption has almost dropped below the detection threshold.

3.2. *Velocity Structure*

In Figures 3*a* and 3*b* we present two different kinds of structures that we found to be responsible for prominent

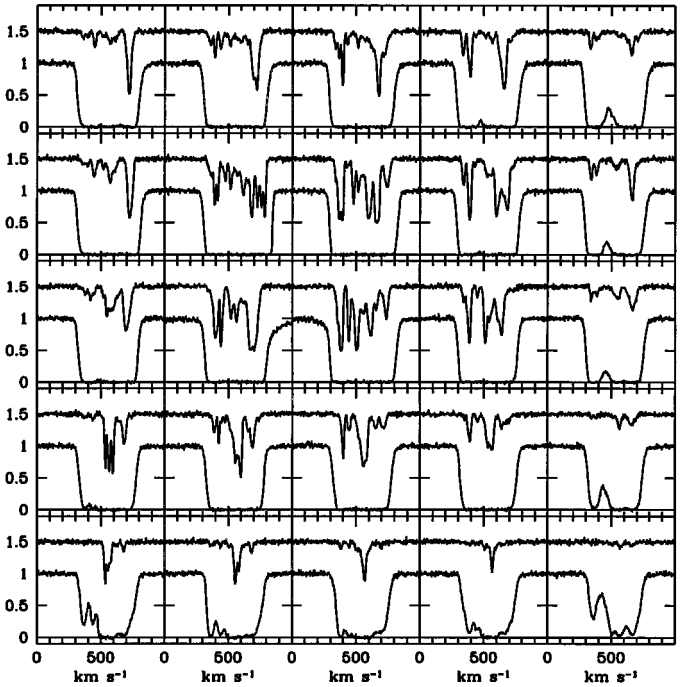

FIG. 2.—C IV and H I absorption for a mosaic of lines of sight around a filamentary structure at $z = 3$. H I and C IV absorption are shifted relative to each other by 0.5. Only the λ1548 line of the C IV doublet is shown. The proper distance between neighboring panels is 10 kpc.

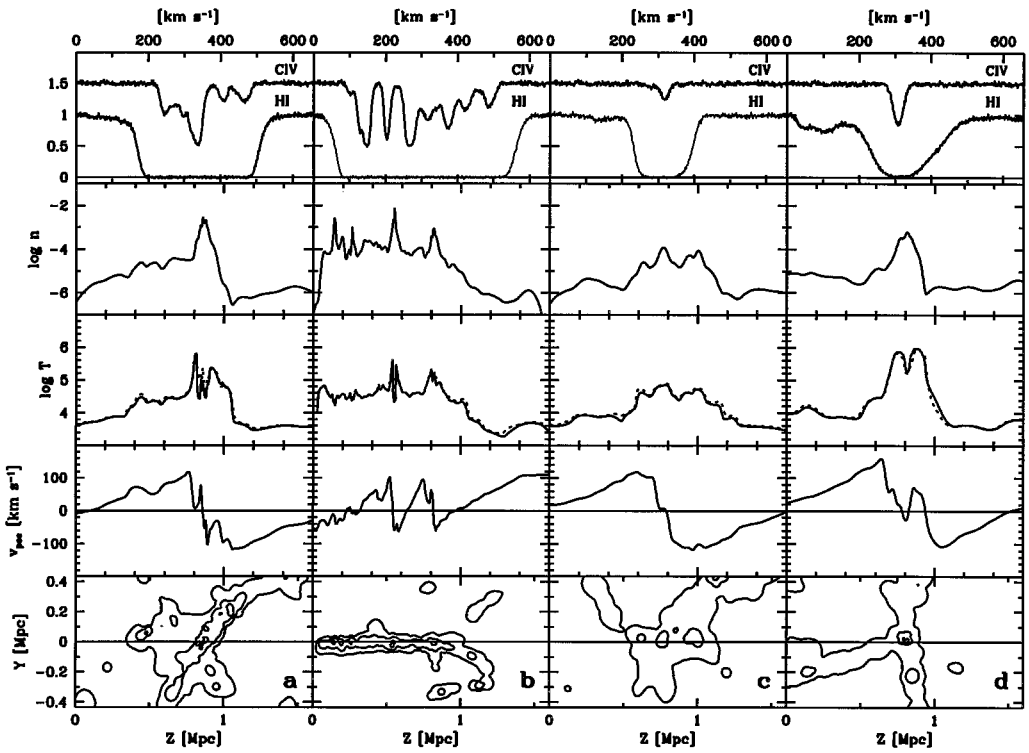

FIG. 3.—Top panels show C IV and H I absorption along selected lines of sight at $z = 3$. The signal-to-noise ratio is 50, the instrumental broadening 8 km s^{-1}, and the bin size 2 km s^{-1}. Only the λ1548 line of the C IV doublet is shown. The next three panels show from top to bottom the corresponding total gas density, H I– (*solid curve*) and C IV– (*dashed curve*) weighted temperatures and the peculiar velocity profile. The bottom panels show contour plots of the C IV density in a plane containing the LOS. The spacing of the contours is 2 dex.

clusters of narrow C IV absorption lines. The four upper panels show the absorption, the density, the C IV– and H I–weighted temperatures, and the velocity profile along the LOS. The bottom panels contain C IV density contour maps. The contour plot and the density profile of Figure 3*a* show that the LOS penetrates a single clump. The temperature is clearly enhanced above the ionization equilibrium temperature, and the complicated temperature profile is responsible for the cluster of C IV lines. The object is obviously not dynamically relaxed. Figure 3*b* shows a LOS along a filamentary structure. The alignment of 5 to 7 well separated clumps, none of which has a circular velocity larger than about 100 km s^{-1}, is responsible for the prominent C IV cluster that extends over 500 km s^{-1}. The broadest and most complex absorption features found in our simulations are produced by such an alignment of dense clumps along filaments.

3.3. *Abundance Determinations*

Determining metal abundances from QSO absorption lines requires at least one pair of ionic species occupying the same spatial region and experiencing the same physical conditions. For low–column density systems, however, there is often only the C IV/H I ratio available. As shown in Figure 1*a*, for the equilibrium case with temperatures of about 10^4 K, there is a broad peak in the C IV/H I column density ratio, log (C IV/H I) ~ [C/H], which extends over 2–3 orders of magnitude in density. Cowie et al. (1995) therefore infer [C/H] = −3 to −2 from their measured C IV/H I column density ratios of about 10^{-3} to 10^{-2}. For our simulations, we find that this assumption generally gives reasonable results. However, as shown in Figure 3*d*, for some LOSs this reasoning can fail by a large margin. Despite the fact that [C/H] = −2, the C IV column density here is only a factor of 8 smaller than the H I column density. These rather rare LOSs pass through the hot atmospheres of dense clumps with gas temperatures close to 3×10^5 K, where the C IV/H I ratio reaches a maximum for collisionally ionized gas (see Fig. 1*a*).

4. DISCUSSION AND CONCLUSIONS

We have demonstrated that LOSs through regions of ongoing galaxy formation can produce C IV absorption complexes very similar to those actually observed. The individual C IV components are related to protogalactic condensations (PGCs) with baryonic masses of about 10^9 $M_\odot$ and radii of about 5–10 kpc.

The PGCs are in a variety of dynamical states. Velocity dispersions in the C IV absorption system of a few hundred kilometers per second are often due to small-scale motions of bound objects, while larger velocities usually arise from the large-scale expansion of the universe and the fortuitous orientation of the LOS along an expanding filament. This interpretation avoids the difficulties associated with accounting for systems with velocity extent in excess of 500 km s^{-1} in terms of galaxy clusters or clouds orbiting in massive halos at these high redshifts (see also Pettini et al. 1983 and Morris et al. 1986).

If we choose a LOS through the very center of a PGC, the H I column density easily exceeds 10^{20} cm^{-2}. Thus, our findings may also be relevant for an understanding of damped Lyα systems. The observed component structure of higher ions associated with damped Lyα systems is very similar to those of nondamped C IV systems. The main difference between C IV–"only" and damped Lyα systems could thus be one of impact

parameter, implying a possible unified picture in which both are caused by groups of PGCs. However, for a rigorous investigation of this question, optical depth effects would have to be taken into account. Evidence for damped Lyα systems as small as the PGCs discussed here comes from observational work of of Møller & Warren (1995; Warren & Møller 1995; Wolfe 1995) and theoretical work by Kauffmann (1996).

The complex component structures arise from density and temperature profiles that vary strongly along the LOS. The assumption that the temperature takes the photoionization equilibrium value, often made in photoionization models, will fail in such cases (see also Miralda-Escudé & Rees 1993). Even for a correctly determined density, the fraction of neutral hydrogen is then systematically overestimated (Haehnelt, Rauch, & Steinmetz 1996). This can lead to severe underestimates of the cloud size along the LOS and might explain the very small C IV cloud sizes of $\sim$100 pc inferred by Cowie et al. (1995). Abundance determinations that assume the gas to be close to the photoionization equilibrium temperature should generally give acceptable abundances. Nevertheless, abundance determinations on the basis of C IV/H I column density ratios alone should be considered with some caution.

Although very idealized, a homogeneous metal contamination of the intergalactic medium with [C/H] ~ -2 leads to an astonishingly good representation of the observed C IV absorption. The appearance of the absorption-line complexes is determined mainly by the temperature and ionization structure of the density maxima and by the large-scale dynamics of the PGC groups. Thus, we expect that our results will not change much, if the metals are not homogeneously distributed.

We conclude that the gas physics and the mass scales included in our simulations of regions of ongoing galaxy formation are sufficient to recover the basic properties of observed C IV absorption systems.

We thank Martin Rees and Simon White for very helpful comments and Gary Ferland for making CLOUDY available to us. M. R. acknowledges instructive conversations with Bob Carswell, Len Cowie, Esther Hu, Palle Møller, Ray Weymann, and Wal Sargent, and is grateful to NASA for support through grant HF-01075.01-94A from the Space Telescope Science Institute, which is operated by the Association of Universities for Research in Astronomy, Inc., under NASA contract NAS5-26555. Support by NATO grant CRG 950752 and the "Sonderforschungsbereich 375-95 für Astro-Teilchenphysik der Deutschen Forschungsgemeinschaft" is also gratefully acknowledged. M. G. H. thanks Wal Sargent and Caltech for hospitality.

REFERENCES

Bergeron, J. 1986, A&A, 155, L8
Bergeron, J., & Boissé, P. 1991, A&A, 243, 344
Cen, R., Miralda-Escudé, J., Ostriker, J. P., & Rauch, M. 1994, ApJ, 437, L9
Cowie, L. L., Songaila, A., Kim, T.-S., & Hu, E. 1995, AJ, 109, 1522
Ferland, G. J. 1993, University of Kentucky Department of Physics and Astronomy Internal Report
Haehnelt, M. G., Rauch, M., & Steinmetz, M. 1996, in preparation
Hernquist, L., Katz, N., Weinberg, D. H., & Miralda-Escudé, J. 1996, ApJ, 457, L51
Kauffmann, G. A. M. 1996, in Cold Gas at High Redshift, ed. M. Bremer, P. Van der Werf, & C. Carilli (Dordrecht: Kluwer), in press
Lake, G. 1988, ApJ, 327, 99
Lanzetta, K. M., Bowen, D. V., Tytler, D., & Webb, J. K. 1995, ApJ, 442, 538
Miralda-Escudé, J., & Rees, M. J. 1993, MNRAS, 260, 624
Mo, H. J. 1994, MNRAS, 269, L49
Møller, P., & Warren, S. J. 1995, in Galaxies in the Young Universe, ed. H. Hippelein, K. Meisenheimer, & H.-J. Roeser (Heidelberg: Springer), 88
Morris, S. L., Weymann, R. J., Foltz, C. B., Turnshek, D. A., Shectman, S., Price, C., & Boroson, T. A. 1986, ApJ, 310, 40
Navarro, J. F., Frenk, C. S., & White, S. D. M. 1995, MNRAS, 275, 56
Petitjean, P., Mücket, J. P., & Kates, R. E. 1995, A&A, 295, L9
Pettini, M., Hunstead, R. W., Murdoch, H. S., & Blades, J. C. 1983, ApJ, 273, 436
Sargent, W. L. W., Boksenberg, A., & Steidel, C. C. 1988, ApJS, 68, 539
Steidel, C. C. 1990, ApJS, 74, 37
———. 1995, in Proc. ESO Workshop, QSO Absorption Lines, ed. G. Meylan (Heidelberg: Springer), 139.
Steinmetz, M. 1996, MNRAS, 278, 1005
Tytler, D., Fan, X.-M., Burles, S., Cottrell, L., Davis, C., Kirkman, D., & Zuo, L. 1995, in Proc. ESO Workshop, QSO Absorption Lines, ed. G. Meylan (Heidelberg: Springer), 289
Vedel, H., Hellsten, U., & Sommer-Larsen, J. 1994, MNRAS, 271, 743
Warren, S. J., & Møller, P. 1995, in IAU Symp. 171, New Light on Galaxy Evolution, (Heidelberg: Springer), in press
Wolfe, A. M. 1995, in Proc. ESO Workshop, QSO Absorption Lines, ed. G. Meylan (Heidelberg: Springer), p. 13
York, D. G. 1988, in Proc. of the QSO Absorption Line Meeting, Baltimore, 1987, QSO Absorption Lines: Probing the Universe, ed. C. Blades, D. Turnshek, & C. A. Norman (Cambridge: Cambridge Univ. Press), 227